Research Article | Vol. 33, No. 25 / 15 Dec 2025 / Optics Express 53182
Optics EXPRESS

Four-wave mixing simulation in weakly nonlinear Bragg gratings using the grating dispersion operator in the nonlinear Schrödinger equation

TIMOTHÉ DAVID,[1,*] PASCAL KOCKAERT,[2] AND STÉPHANE CLEMMEN[1,2,3]

[1] *Laboratoire d'Information Quantique, Université libre de Bruxelles, 50 Av. F. D. Roosevelt, CP 224, 1050 Brussels, Belgium*
[2] *OPERA-Photonique, Université libre de Bruxelles, 50 Av. F. D. Roosevelt, CP 194/5, 1050 Brussels, Belgium*
[3] *Photonics Research Group, Department of Information Technology, Ghent University-imec, Technologiepark-Zwijnaarde 126, 9052 Ghent, Belgium*
[*] *timothe.david@ulb.be*

Abstract: While the nonlinear Shrödinger equation (NLSE) and its solving via the split-step Fourier method are well established when studying the Kerr interactions in waveguides, it is typically not applied when modeling a nonlinear interaction in a Bragg grating (BG). In that specific case, the solving of a set of coupled equations is preferred as they form the natural framework to deal with co- and contra-propagating waves. This, however, has limitations for input spectra much larger than this bandgap, e.g., for frequency combs or multispectral pump schemes. In order to deal with those in a Bragg grating, we adapt the usual NLSE solving via split-step Fourier by embedding the Bragg resonance into the dispersion operator. Although it requires that the total nonlinearity along the propagation remains moderate, i.e., the nonlinear phase shift $\gamma PL < 2\pi$, and the pump(s) frequency(ies) to be outside of the bandgap, this modeling allows us to retrieve established results and points towards the BG ability to tune and quench four-wave mixing processes.

1. Introduction

Four-wave mixing (4WM) is a nonlinear process capable of changing the wavelength and/or bandwidth of quantum fields in a noiseless and phase preserving way [1] (via Bragg Scattering-4WM), of generating light squeezing [2] and of classical data processing [3,4]. For quantum applications such as Bell state generation or squeezing, and some classical ones such as Kerr comb and supercontinuum generation, some of the waves involved may grow from vacuum fluctuations which are intrinsically broadband (white). In simple cases, predictions can be made analytically. More generally, the nonlinear Schrödinger equation (NLSE) can be solved numerically for many four-wave mixing processes via the split-step-Fourier method [5]. However, when considering several spectrally separated narrowband pulses or resonant structures (such as Bragg gratings), the coupled mode theory and coupled mode equations are used for the case of quasi-CW (Continuous Wave) pulses [5] whereas the coupled NLSE are used for spectrally extended pulses [6,7].

Focusing on the case of Bragg gratings where the coupled mode theory is typically applied between co and contra-propagative modes [8], the inclusion of the Kerr nonlinearity is possible; and solving using finite difference [9], a split-step method [10], or heuristically [11] have been shown to reproduce the behaviour of experimental measurements [12]. Interestingly, when considering a narrowband pulse whose central frequency is larger than the Bragg resonance, the

#572984 https://doi.org/10.1364/OE.572984
Journal © 2025 Received 9 Jul 2025; revised 15 Oct 2025; accepted 22 Oct 2025; published 10 Dec 2025

Optics EXPRESS

coupled mode equations have been showed to be well-approximated by a NLSE using the method of multiple scales [13]. However these methods are not suited to the study of the broadband parametric processes involving frequencies that can be inside, close and far away from the Bragg resonance.

The use of Bragg gratings in nonlinear optics has been explored as early as the 90's for the creation of solitons [14–16]. While Bragg gratings are mainly known for their reflective and dispersive properties that are exploited for spectral filtering [8] and dispersion management [17] respectively, their application to phase-matching tuning has been reported for a variety of processes [18], such as phase sensitive processes [19], quasi-phase matched four-wave-mixing in a hybrid structure [20] and enhancement of on-chip optical parametric amplification [21]. In this context, Bragg gratings complement other dispersion engineering techniques such as waveguide geometry [22,23], overlays, atomic resonances [24], photonic crystals [25] or coupled-resonator optical waveguides [26].

Nowadays one can manufacture meter-long fiber Bragg grating [27], or centimeter-long integrated Bragg grating [28] that benefit from the stronger nonlinearities offered by transverse strong confinement, with "à la carte" shapes, strength and length. To take the best advantage of these recent technological developments, it appears that an efficient way to simulate broadband nonlinear propagation in Bragg gratings is necessary. We introduce such a method and perform simulations for several applications.

2. Theoretical background

Similarly to the solving of NLSE, our solving is based on the slowly varying envelope approximation, negligible group velocity walk-off (due to the dispersion) and in its simplest form assumes independence of the effective mode area with respect to wavelength.

In order to model the four-wave mixing in a Bragg grating, we are using a grating dispersion operator in the NLSE that includes both the refractive and reflective effects of the grating on the incident pulse but neglect the nonlinear coupling with the backward reflected light. This allows to model the nonlinear propagation of multichromatic quasi-CW inputs as well as more spectrally extended pulses in a grating, when the reflected power is low. Although it turns out a similar idea has already been proposed almost two decades ago for continuum generation [29], we went further in the mathematical development: we quantified the domain of validity of our grating dispersion expression and showed it is an improved version of the one presented in [29].

2.1. Nonlinear Schrödinger equation in absence of a Bragg grating

The nonlinear Schrödinger equation (NLSE) can be written

$$\frac{\mathrm{d}A(z,t)}{\mathrm{d}z} = (D+N)A\ , \tag{1}$$

with D the dispersion operator and N the nonlinear operator. A is the envelope of the electric field which has a propagation constant β. Assuming D and N are invariant over a small step dz, and assuming that they commute (Baker-Hausdorff-Campbell approximation) provides (with error scaling with dz^3 [5]):

$$A(z+dz) \approx \exp(\frac{dz}{2}N)\exp(dzD)\exp(\frac{dz}{2}N)A(z)\ . \tag{2}$$

With this approximation, $A(z+dz)$ can be solved numerically via the SSF method [30] consisting of alternating nonlinear propagation in the temporal domain and dispersive propagation in the spectral domain.

Optics EXPRESS

The nonlinear operator $N = i\gamma|A|^2$, with γ the nonlinear coefficient. The dispersion operator D is well approximated (in a waveguide) by a polynomial of temporal derivatives. It is expressed in the spectral domain:

$$\tilde{D}(\omega) = i[\beta(\omega) - \beta_0 - \beta_1(\omega - \omega_{\text{ref}})] \,, \tag{3}$$

for a reference frame moving at velocity $1/\beta_1$, with β_j being the j-th derivative of β evaluated at the reference frequency ω_{ref} [5]. In this work we replaced the constant dispersion operator $\tilde{D}(\omega) = i[\beta(\omega) - \beta_0 - \beta_1(\omega - \omega_{\text{ref}})]$ of the waveguide by a z-dependent dispersion operator $\tilde{D}_{\text{BG}}(z, \omega) = C'(z, \omega) - i[\beta_1(\omega - \omega_{\text{ref}})]$. By choosing the adequate $C'(z)$ (section 2.3.1) our simulations show that the grating dynamic onto the nonlinear field can be modeled, providing no intense field is reflected (to keep N unchanged) and the nonlinear phase remains moderate (section 2.2.2). We then use this model to numerically investigate other cases of interest.

2.2. *Grating dispersion, wave vector kick and the intermediate nonlinear regime*

In this part we introduce the wave vector dispersion q often used in the coupled mode theory and that will play a crucial role in the grating dispersion operator.

2.2.1. Usual grating parameters, dispersion and wave vector kick

Let us consider a propagating mode of the waveguide characterized by an effective index n_{eff} and thus a wave vector $\beta_{\text{wg}} = n_{\text{eff}}\frac{\omega}{c}$. In a waveguide Bragg grating with a small index modulation $n_{\text{gr}}(z) = n_{\text{eff,mean}} + \delta n(z)$ [8], the propagation remains unaltered far away from the Bragg resonance $\lambda_{\text{Bragg}} = 2n_{\text{eff,mean}}\Lambda$ with Λ the period of the modulation. It doesn't matter here how the grating is implemented, it can be a direct modulation of the index in the waveguide core (typical from FBGs), in the cladding (typical from tilted FBGs) or a grating evanescently coupled to the waveguide (typical of nanophotonic waveguides). Typical values for Bragg gratings are $n_{\text{eff,mean}} \in [1.4, 3.4]$ and $\delta n \in [10^{-7}; 10^{-2}]$. This modulation can generally be of any form $\delta n(z) = \sum_{j\in\mathbb{Z}} \delta n_j e^{i\frac{2\pi j}{\Lambda}z}$ but we will consider only the first order for simplicity. The index modulation $\delta n(z)$ is linked to the grating strength κ and the Bragg wavelength λ_{Bragg} through $\kappa \approx \frac{\pi\delta n}{\lambda_{\text{Bragg}}}$. The total wave vector including both the contribution of the waveguide and the Bragg resonance can be expressed as [17]:

$$\beta_{\text{wg-gr}}(\omega) = \frac{\pi}{\Lambda} \pm \sqrt{\left(\beta_{\text{wg}}(\omega) - \frac{\pi}{\Lambda}\right)^2 - \kappa^2} \,. \tag{4}$$

Exactly at the resonance we have $\frac{\pi}{\Lambda} = \beta_{\text{wg}}(\lambda_{\text{Bragg}}) \equiv \beta_{\text{Bragg}}$. The difference $\delta(\omega) = \beta_{\text{wg}}(\omega) - \beta_{\text{Bragg}}$ is called the wave vector detuning [17]. Finally, we can introduce the parameter $q_{\text{linear}}(\omega) = \pm\sqrt{\delta(\omega)^2 - \kappa^2}$ [17] in order to use a simpler expression for the dispersion of the grating :

$$\beta_{\text{wg-gr}}(\omega) = \beta_{\text{Bragg}} + q_{\text{linear}}(\omega) \,. \tag{5}$$

This parameter $q_{\text{linear}}(\omega)$ is the one typically used in the coupled mode theory. Its sign is chosen so that its asymptotic behaviour is consistent with the physics: without grating ($\kappa \approx 0$) we should retrieve the waveguide detuning ($q_{\text{linear}} \approx \delta$), or equivalently the waveguide wave vector, i.e. $\beta_{\text{wg-gr}} \approx \beta_{\text{wg}}$. Indeed, when $\delta \gg \kappa$, $q_{\text{linear}} \approx \sqrt{\delta^2} = \pm|\delta|$. Hence, $\beta_{\text{wg-gr}} = \beta_{\text{Bragg}} + q_{\text{linear}} \approx \beta_{\text{Bragg}} \pm |\delta|$ while $\beta_{\text{wg}} = \beta_{\text{Bragg}} + \delta$. Having consistent physics hence requires to use a positive q_{linear} for frequencies corresponding to positive δ and a negative one for frequencies giving negative δ. We conveniently also define a *wave vector kick* outside the bandgap as $k(\omega) = q_{\text{linear}}(\omega) - \delta(\omega) = \sqrt{\delta(\omega)^2 - \kappa^2} - \delta$. This parameter quantifies the influence of the grating on the waveguide wave vector. It is positive for frequencies lower than the Bragg frequency, negative otherwise, and its magnitude is maximal at the resonance edges, i.e. when

Optics EXPRESS

$|\delta| = |\kappa|$ (corresponding to $q_{\text{linear}} = 0$ and $k = \pm\kappa$), see Fig. 1. The maximum kick is hence related to the index modulation and the effective index, as expressed in Eq. (6)

$$\max\left(\left|\frac{k}{\beta_{\text{wg}}}\right|\right) = \frac{\delta n}{2n_{\text{eff}}}, \tag{6}$$

and behaves as expected: a deeper modulation has a stronger effect and results in a stronger kick. Equation (6) allows to quickly evaluate if a grating is relevant to affect the phase matching of a particular parametric process. Indeed, the wave vector kick k must be at least comparable to the phase mismatch $\Delta\beta_{\text{wg}}$ of the nonlinear process under investigation :

$$\Delta\beta_{\text{wg}} \leq \frac{\delta n}{2n_{\text{eff}}}\beta_{\text{Bragg}}\,. \tag{7}$$

As an illustration, for a Bragg grating with $\delta n_1 = \delta n/2 \approx 2.10^{-3}$ in a nanophotonic waveguide with $n_{\text{eff}} \approx 2$, we can expect a simple Bragg grating to have a relevant influence on the phase if the mismatch $\Delta\beta_{\text{wg}} \approx \frac{1}{1000}\beta_{\text{Bragg}}$. This order of magnitude can be encountered in third-order nonlinear phenomena (such as Bragg-scattering four-wave mixing) but is very (very) unlikely to happen in second-order nonlinear phenomena. That is why the focus is made on third-order processes in this work.

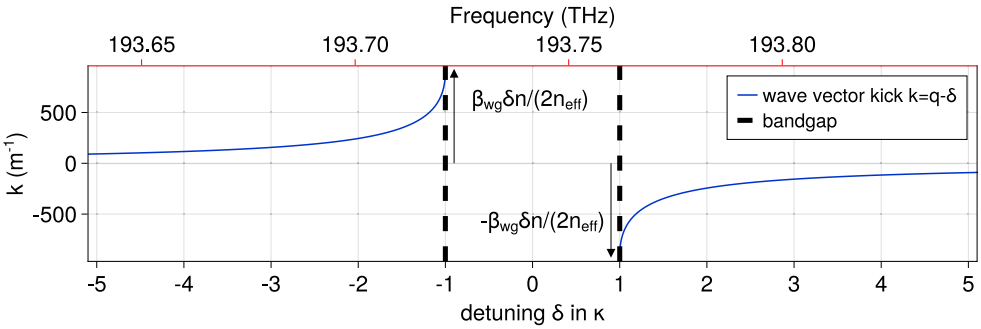

Fig. 1. Wave vector kick $k = q - \delta$ in a grating (blue line) close to the bandgap (black dashed lines) as a function of the incoming frequency. Outside (resp. inside) of the bandgap q is purely real (resp. imaginary). Here, $\delta n_1 = \delta n/2$ with $\delta n = 4.49 \times 10^{-4}$, $\lambda_{\text{Bragg}} = 1548.48$ nm.

2.2.2. Intermediate nonlinear regime: linear grating and nonlinear effects

It is well known [14] that nonlinear effects such as optical bistability and bandgap shifting can occur in Bragg gratings at high optical intensities. Here we focus on an intermediate nonlinear regime where the nonlinear phase $\phi_{\text{nl}} = \gamma PL < 2\pi$ with the nonlinear parameter γ, the propagation length L and the optical peak power P. We shall demonstrate that this condition is enough to neglect the impact of the nonlinearity on the grating wave vector kick. For that, let us consider the fraction f of the field that is reflected in presence of that nonlinearity, the term q_{linear} in Eq. (5) becomes q_{total} [17]:

$$q_{\text{total}} = \frac{-\kappa(1-f^2)}{2f} - \frac{\gamma P}{2}\frac{1-f^2}{1+f^2} \quad \Longrightarrow \quad |q_{\text{total}} - q_{\text{linear}}| = \left|\frac{\gamma P}{2}\frac{1-f^2}{1+f^2}\right| \leq \frac{\gamma P}{2}, \tag{8}$$

where we used $q_{\text{linear}} = q_{\text{total}}(\gamma = 0)$ and the last inequality is obtained using $\frac{1-f^2}{1+f^2} \in [-1, 1]$ irrespective of the details of the grating or the wavelength detuning between the field and the

Optics EXPRESS

grating resonance. Since we care about situations of efficient nonlinear interactions demanding the phase mismatch $\Delta\beta \leq \frac{\pi}{L}$, the condition for validity of our study as

$$|q_{\text{total}} - q_{\text{linear}}| \leq \frac{\gamma P}{2} < \frac{\pi}{L}\,, \tag{9}$$

is sufficient for approximating q_{total} by q_{linear}. Rewriting $\frac{\gamma P}{2} < \frac{\pi}{L}$ to exhibit the nonlinear phase shift gives the following condition

$$\gamma P L < 2\pi\,. \tag{10}$$

Equation (10) defines the "intermediate nonlinear regime": the maximal reasonable nonlinear phase shift that allows to work with q_{linear} instead of q_{total}, i.e., where Eq. (7) applies. For instance, an optimal wavelength conversion via the process of Bragg scattering four-wave mixing [31] requires $P = \frac{\pi}{4\gamma L}$ which corresponds to $\gamma P L = \frac{\pi}{4} \ll 2\pi$ and $|q_{\text{total}} - q_{\text{linear}}| \leq \frac{\pi}{8L} \ll \frac{\pi}{L}$.

2.3. Dispersion operator for forward propagating field in a Bragg grating

Following this "intermediate nonlinear regime" assumption, we derive a new dispersion operator that accounts for the linear grating dispersion and reflection. We will refer to it as the grating dispersion operator. By construction this operator exactly reproduces the grating linear behaviour. When compared (in Supplement 1) to previous similar attempts, it is shown to be more precise.

2.3.1. Deriving the grating dispersion operator D_{BG}

A proper modeling of a Bragg grating requires to include a z-dependency in the D operator. Although the usual dispersion operator D can be tuned via its parameters to account for the presence of a grating, the validity of that approach is restricted to cases where all the waves are in the direct vicinity of the bandgap [13]. In the more general case, the form of the dispersion operator must be modified. Since the dispersive step in NLSE is performed in the spectral domain, we can focus on a spectral expression for a z-dependent dispersive operator $D(z, \omega)$. We note that a standard case where $D(\omega)$ is z-independent gives rise to a z-independent wave constant $\beta(\omega)$ (see Eq. (3)) and this does not allow for having an operator that describes correctly the grating induced dispersion (see Supplement 1). That is why a generalized approach is required.

The previously established "intermediate nonlinear regime", in Eq. (10), indicates the maximum nonlinearity for the linear grating description to remain valid. Hence, we will exhibit an expression for the grating dispersion operator $D(z, \omega)$ relying on the linear wave vector dispersion $q^2_{\text{linear}} = \delta^2 - \kappa^2$. Looking for a z-dependent operator $D(z, \omega)$ in linear regime (Eq. (1) with $N \equiv 0$) implies that

$$\frac{dB(z,\omega)}{dz} = D(z,\omega)B(z,\omega)\,, \tag{11}$$

with the spectral envelope $B(z, \omega)$ being related to the temporal envelope $A(z, t)$ in the frame moving at the group velocity $1/\beta_1$ by $B(z, \omega) = \text{FT}[A(z, t)]$. To simplify the treatment, we go back into the immobile frame by introducing $b(z, \omega)$ so that $b(z, \omega) = B(z, \omega) \times \exp(i\beta_1(\omega - \omega_{\text{Bragg}})z)$ if the Bragg frequency is taken as the reference frequency. Computing $\frac{db}{dz}$ by using Eq. (11) gives

$$\frac{db(z,\omega)}{dz} = C'(z,\omega)b(z,\omega)\,, \tag{12}$$

where $C'(z, \omega)$ is given by $C'(z, \omega) = D(z, \omega) + i\beta_1(\omega - \omega_{\text{Bragg}})$. A function $C(z, \omega)$ whose first derivative obeys Eq. (12) leads to

$$b(z,\omega) = \exp(C(z,\omega))b(0,\omega), \tag{13}$$

where the case $C(z, \omega) = i\beta(\omega)z$ corresponds to the usual propagation constant description. The Eq. (13) is a general transfer function equation. Hence, an analytical linear dispersion operator

Optics EXPRESS

for the NLSE can be obtained for any system that has an analytic expression of its transfer function (still assuming our intermediate nonlinear regime and low reflected power if relevant). In our case, we derive the function $C(z,\omega)$ and $C'(z,\omega)$ for a Bragg grating using the transmitted amplitude transfer function

$$\tau(\omega,z) = \frac{q_\omega \cos(q_\omega z) + i(\delta + r_\omega \kappa)\sin(q_\omega z)}{q_\omega}\,, \tag{14}$$

for a linear grating of length L, with $q_\omega = q_{\text{linear}}(\omega)$ and $r_\omega = \frac{i\kappa\sin(q_\omega L)}{q_\omega\cos(q_\omega L) - i\delta\sin(q_\omega L)}$ the grating reflection [8,32]. The details of the derivation are presented in Supplement 1. This transfer function directly takes into account the influence of the backward field introduced in the coupled-mode theory and leads to

$$C(z,\omega) = \ln(\tau(z,\omega))\,, \tag{15}$$

with ln a complex logarithm, and thus

$$C'(z) = q_\omega \frac{i(\delta + r_\omega\kappa)\cos(q_\omega z) - q_\omega \sin(q_\omega z)}{q_\omega\cos(q_\omega z) + i(\delta + r_\omega\kappa)\sin(q_\omega z)}\,. \tag{16}$$

Finally, using the relation between C' and D, we obtain the grating dispersion operator for the spectral envelope $B(z,\omega)$ in the moving frame:

$$D_{\text{BG}}(z,\omega) = C'(z,\omega) - i\beta_1(\omega - \omega_{\text{Bragg}})\,. \tag{17}$$

Far from the grating resonance $q_\omega \approx \delta$ and $C'(z) \approx i\delta = i(\beta - \beta_0)$ so that the grating dispersion operator coincides with the usual waveguide dispersion operator and similarly if there is no grating, $q_\omega = \delta$ and $C'(z) = i\delta$.

A previous attempt to use a grating dispersion operator has been performed by a direct use of the grating dispersion q_ω and by treating the bandgap as an ideal one, meaning the backward propagating field from the coupled mode theory was completely ignored to compute the value of the forward propagating field [33]. Using our notation, it corresponds to $D_{\text{BG,ideal}} = iq_\omega - \beta_1(\omega - \omega_{\text{Bragg}})$. Another attempt consisted in treating the grating response (hence $C(z,\omega)$) as an atomic resonance independent of z [29], corresponding to a z-independent operator $D_{\text{BG}}(z,\omega) = D_{\text{BG}}(\omega) = C(L,\omega) - i\beta_1(\omega - \omega_{\text{Bragg}})$. The details of the comparison between $D_{\text{BG}}(z,\omega), D_{\text{BG}}(\omega)$ and $D_{\text{BG,ideal}}$ are developed in Supplement 1. Although these previous attempts offer greater simplicity and fast computation, $D_{\text{BG}}(z,\omega)$ is the only operator that allows the numerical retrieval of the grating response in amplitude and phase.

2.4. Numerical implementation

Interested in multi-wavelength interactions in the Bragg grating, we model the input pulses with a single field with different frequency components and solve the NLSE using the SSF method with the dispersion operator of Eq. (17). The reference frequency ω_{Bragg} is chosen to be the Bragg frequency as it allows for simpler equation [17]. Because we descirbe the system in the pulse frame, we need to ensure that we can neglect the group velocity mismatch of the different wavelengths (including the one induced by the grating [34]). In practice, this condition requires either long pulses compared to the group velocity mismatch after propagation (few ps is enough in our case where the maximum mismatch is about 0.3 ps/cm) and/or frequencies spectrally close to each other (to minimize the group velocity mismatch). At least one of those is always satisfied hereafter. This approximation also allows for considering a unique Taylor decomposition of the dispersion (e.g., to 4^{th} order) that is valid for our wavelengths interval.

Optics EXPRESS

For transform-limited Gaussian input fields of respective (temporal) amplitudes A_i, centered around the frequencies ν_i with durations (full width at half maximum) t_i, the corresponding single pulse $B(0,\nu)$ that enters the NLSE is given in the frequency domain by

$$B(0,\nu=\frac{\omega}{2\pi}) = \sum_i N_i \exp\left\{-\left(\frac{\pi(\nu-\nu_i)t_i}{2\sqrt{\ln(2)}}\right)^2\right\}, \tag{18}$$

with $N_i = A_i t_i \sqrt{\frac{\pi}{\ln(2)}}\frac{1}{2\delta t}$ where δt is the time sampling i.e. the ratio between the numerical time window and the number of time samples. This normalization is such that $|B(z,\omega)|^2$ is the discrete Fourier Transform (with unit in W/Hz) of the physical time envelope whose intensity $|A(z,t)|^2$ is in W. We assert using the grating dispersion operator $D(z,\omega)$ over the "merged" single pulse $B(0,\omega)$ from Eq. (18) is able to account for the grating influence over a parametric process, reduced to a single NLSE.

A numerical implementation of this theoretical model requires to substitute the usual dispersion operator $D(\omega)$ in the SSF scheme by the z-dependent grating dispersion operator $D_{\mathrm{BG}}(\omega,z)$. Then, technical considerations are identical to other SSF implementations [5]. A GPU implementation of the grating dispersion operator into a SSF scheme that solves the NLSE can be found in [35]. Every nonlinear propagation simulation made in this paper uses this code.

With the theory established, we now look at simulation results for various cases.

3. Case study

In order to check the consistency of our approach, we first apply our model to previously reported experimental (section 3.1) and theoretical results (section 3.2): the first one involves the nonlinear pulse propagation of single pulse in the vicinity of a Bragg Grating [12], the other involves a non-degenerate 4WM in absence of a Bragg grating [31]. Both examples are typically modeled via coupled equations. Then, we apply our model first to a wavelength conversion process to display the increase of tunability due to the Bragg grating, and to the generation of wavelength-degenerate photon pairs where the Bragg grating purifies noisy processes or conveniently push the optimal bandwidth away from the pump wavelength. All these simulations are in the intermediate nonlinear regime defined by Eq. (10).

3.1. Single pulse propagation in Bragg gratings

The single pulse propagation near a Bragg resonance in fiber Bragg gratings has been studied both experimentally and numerically in 1997 [12]. The model used at the time was based upon nonlinear coupled mode equation. Using a standard value for the nonlinear coefficient for fibers, the nonlinear phase shift γPL from this scenario can be evaluated to be smaller than 1, hence Eq. (10) is true and we can use our model. We compare our simulation to the one from Ref. [12], where the simulation is also backed up experimentally.

Figure 2(left) shows the temporal compression due to the propagation of a single pulse in a fiber Bragg grating when the Kerr nonlinearity becomes significant [12]. It is directly linked to the Bragg soliton phenomenon [12,36] resulting from the balance between the nonlinearity and the grating dispersion on the upper band edge of the bandgap ($\delta>\kappa$) . Our prediction (right panel of Fig. 2) reproduces both the compressed shape and the delay of the output pulse when using parameters from [12] and standard values for the dispersion of the fiber and effective area (the authors of [12] refer to germanosilicate fibers [37] with a core diameter about 5µm without providing more details). Since the exact dispersion and mode area are unknown, they may explain the highest amplitude of the second peak observed in our simulation versus the one from Ref. [12].

Optics EXPRESS

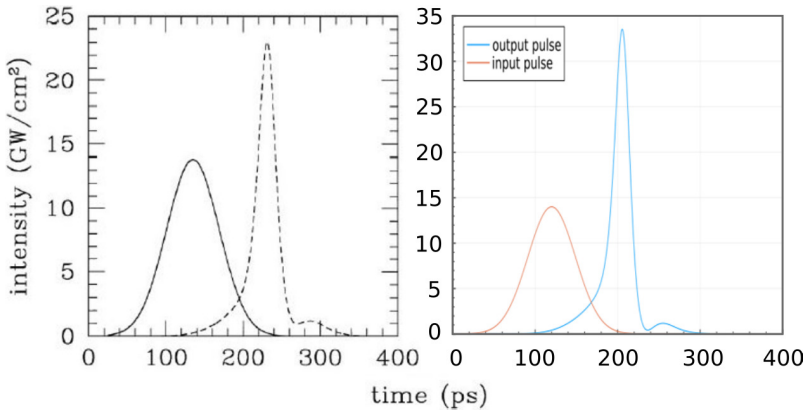

Fig. 2. Comparison of the results from [12] using coupled mode equations (left) and our simulations using dispersion extended NLSE (right). Parameters for the figure on the left are: $\kappa \approx 10$ cm^{-1}, $L = 3.5$ cm, input pulse FWHM = 80 ps, $I = 14$ GW/cm^2, $\delta = 13.2$cm^{-1} with a Bragg wavelength $\lambda_B = 1053.175$ nm. Parameters for the figure on the right are: $\kappa \approx 10$ cm^{-1}, $L = 3.5$ cm, input pulse FWHM = 80 ps, $I = 14$ GW/cm^2, $\delta \approx 15.8$ cm^{-1} with a Bragg wavelength $\lambda_B = 1053.293$ nm.

Thus, our model seems to accurately reproduce a nonlinear propagation for a single pulse that is spectrally close to the bandgap and experience a complex interplay of nonlinear and dispersive effects. The next step consists in testing our model with several pulses in a nonlinear context.

3.2. *Grating assisted BS-4WM for unity conversion efficiency*

The process of Bragg grating four-wave-mixing (BS-4WM) illustrated in Fig. 3(a) allows for the noiseless conversion of quantum light fields from an initial wavelength to a new one [38]. It is often described via coupled mode theory. For long CW pulses the efficiency η of the conversion defined as the ratio between output idler power $P_i(z = L)$ and input signal power $P_s(z = 0)$ takes the form [31]

$$\eta = |2\gamma PL|^2 \mathrm{sinc}_\pi^2 \left(\frac{L}{\pi} \sqrt{(2\gamma P)^2 + (\frac{\Delta\beta}{2})^2} \right) , \tag{19}$$

when both pump beams are set to be of equal power P, with $\mathrm{sinc}_a(x) = \frac{\sin(ax)}{ax}$. A simple study of η shows that a maximum efficiency is reached for

$$\gamma PL = \frac{\pi}{4} \sqrt{(2n+1)^2 - \frac{(\Delta\beta L)^2}{\pi^2}} , \tag{20}$$

with n a positive integer (this requires $\Delta\beta < \frac{(2n+1)\pi}{L}$) and typically one takes $n = 0$ since it corresponds to the central maximum, which is highly dominant. The ideal scenario with $\Delta\beta \approx 0$ implies $\gamma PL = \frac{\pi}{4}$. Hence we are in the intermediate nonlinear regime (Eq. (10)) that allows us to use our model. Figure 3(g) depict the conversion efficiency η of the BS-4WM configuration illustrated in 3(a) as a function of one of the pump wavelength (λ_1), the other pump (λ_2) and the signal (λ_s) being invariant. The black curve shows the analytical expectation while the big blue dots (resp. tiny deep blue dots) come from our model using D from Eq. (3) (resp. D_{BG} from Eq. (17)) in the NLSE to simulate the nonlinear propagation in a waveguide (resp. a Bragg grating).

One can directly observe that the main lobe is notably higher in the analytical case compared to our simulations. In addition, the efficiency in the grating and in the waveguide differ slightly

Optics EXPRESS

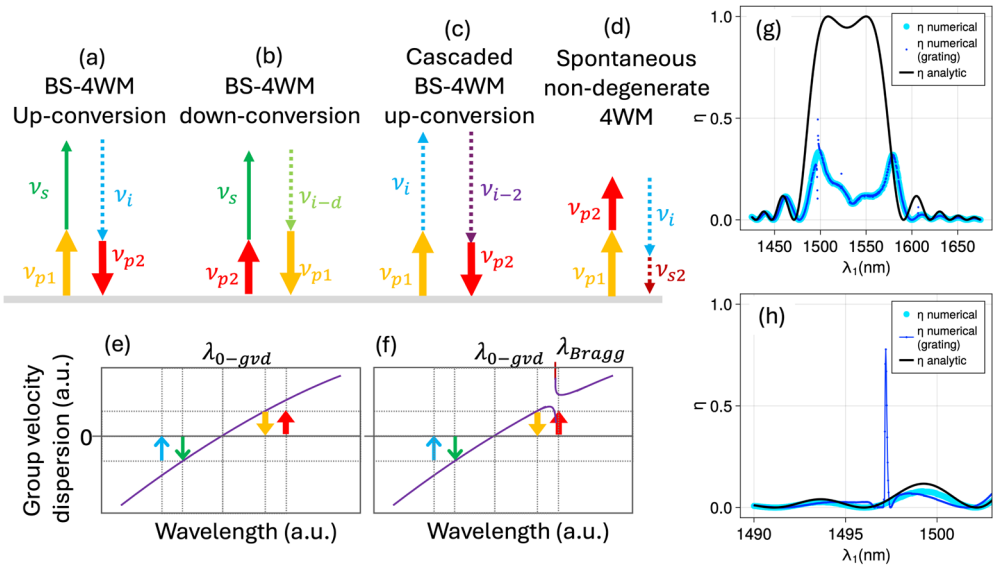

Fig. 3. Bragg scattering four-wave mixing (BS-4WM) and the impact of a dispersive Bragg grating. (a) Energy diagram of the BS-4WM of reference that up-converts an initial field at ν_s to a final frequency ν_i; (b) energy diagram of a competing BS-4Wm that down convert the same initial field at ν_s to a smaller final frequency ν_{i-d}; (c) energy diagram of a competing cascaded process where the BS-4WM up-conversion (a) is followed by a second up-conversion resulting in a final frequency ν_{i-2}; (d) energy diagram of a process of spontaneous 4-wave mixing induced by the two pump beams and may create photons at the the wavelength of interest (here ν_i); (e) typical configuration of a BS-4WM highlighting the importance of the 0-GVD wavelength; (f) modified dispersion curve in the presence of a Bragg grating; (g) BS-FWM conversion efficiency η; (g) BS-4WM efficiency η as a function of one of the pump wavelength λ_1 according to the analytical model (black curve) and according to the numerical simulations accounting competing processes in the absence (light blue) and presence (dark blue) of a Bragg grating; (h) same as (e) for a 10 times longer grating (with 10 times less pump power). Parameters for plot (g) and (h) are: $\lambda_s = 630$ nm and $\lambda_2 = 1550$ nm, and resp. $\kappa L \approx 9$, $\kappa L \approx 90$.

close to $\lambda_1 = 1500$ nm. Let us focus first on the difference between the analytical model and our simulations.

For the analytical model to be valid when the conversion efficiency is close to 100%, extra conditions must be considered [39] because competing processes such as the complementary BS-4WM configuration (Fig. 3(b)), cascaded BS-4WM (Fig. 3(c)) or spontaneous four-wave mixing (Fig. 3(d)) may arise that will effectively reduce the conversion efficiency or add noise. Accounting for these spurious processes via additional coupled equation is possible but cumbersome. In contrast, it is automatically accounted for with the numerical simulation presented here. Hence, Fig. 3(g) illustrates a situation where competing processes are indeed impacting the result. While the analytic model considering only one BS-4WM gives a perfect conversion efficiency, the numerical simulation accounting for the competing processes reveals that the conversion efficiency is reduced below 50%. In practice such a case corresponds to a configuration where the pumps are spectrally close to each others. This explains for instance why in Ref. [40] the optimal efficiency of the desired process is lower than the analytical one when pumps are not depleted. Indeed two BS-4WM are phase-matched, hence decreasing the desired efficiency.

Optics EXPRESS

The way to ensure that one particular BS-4WM process (for definiteness, let say the up-conversion process depicted in Fig. 3(a)) doesn't suffer from competition from other processes is by quenching those other processes. This can be done by imposing a strong phase mismatch [39] to those processes and eventually may demand dispersion engineering. A typical (but not exclusive [41]) configuration for the BS-4WM up-conversion process consists in setting the pump waves and the quantum light fields symmetrically around the 0-GVD wavelength (see Fig. 3(e)), giving equal power for both pump beams $P_1 = P_2 = P = \pi/(4\gamma L) \gg P_s$ (for unity conversion efficiency), having the pump waves temporally longer and thus completely overlapping the signal to be converted, and choosing the interaction length smaller than the inverse of the phase mismatch : $\Delta\beta = \beta(\lambda_1) + \beta(\lambda_s \pm \delta\lambda) - \beta(\lambda_2) - \beta(\lambda_i \pm \delta\lambda) \ll 1/L$. This later condition is necessary when considering the finite bandwidth of the signal. However, it may be incompatible with the targeted strong mismatching of the competing processes. This is where the localized action of the grating on the dispersion may become useful

Indeed in Fig. 3(g), we see that the presence of a Bragg grating can boost the conversion efficiency when one of the pump (at λ_1) is in the close vicinity of the Bragg resonance. This is obviously due to the dispersion the grating induced and that affects all processes involving this pump. It is further evidenced by a decrease of the conversion efficiency on the other side of the Bragg grating bandgap. This effect is magnified in the simulation illustrated in Fig. 3(h) where the accumulated nonlinear phase is unchanged but the length is increased 10-fold. There, the conversion reaches 78% (deep blue) in the grating while being capped at 3% in its absence.

Now that the usefulness of the Bragg grating is evidenced, we are looking at a more systematic metrics improvements.

3.3. BS-4WM with increased tunability

The most interesting case of unity efficient BS-4WM is attained by satisfying the phase matching condition for the process of interest and by imposing a strong phase mismatch to any competing processes involving the same target wavelengths. Such a situation is illustrated in Fig. 4(a) and it shows a quasi linear dependency of one pump wavelength λ_1 onto the other wavelength λ_2 in order to keep unity efficiency for a fixed initial signal wavelength λ_s. The small departure from a perfectly linear behaviour results from the curvature of the second order dispersion curve $\beta_2(\omega) = \frac{\partial^2\beta}{\partial\omega^2}(\omega)$. In practice, this dependency is often a nuisance as it implies that tuning the final idler frequency requires to tune both pump wavelengths in order to keep a good efficiency. This may impose expensive technological choices such as the use of tunable external cavity lasers. In order to quantify this tuning, let us define the tunability of the process as the amount of tuning allowed for one wavelength (λ_2) while fixing the other (λ_1) and keeping the efficiency within 90% of its maximum value.

We show the grating may improve the tuning in Fig. 4(b). The linear behaviour is broken around the Bragg resonance that takes place around 1548 nm. With the grating, we have obtained new pairs (λ_1, λ_2) for which the conversion of λ_s reaches unity. Specifically, to achieve the same tuning of λ_2 than in Fig. 4(a), we need a 2-fold smaller tuning of λ_1. This reduction is due to the strong dispersive effect of the grating around the bandgap. The efficiency is obviously sensitive to the variations of λ_1, but for modern lasers where the central wavelength control is often better than 0.1 pm, it is not an issue. This has 2 consequences, the first is the ability to obtain new idler photon frequencies that are not easily available in a waveguide for the same set of (λ_1, λ_2, λ_s). The second is the improvement of the tunability of λ_2.

The simulation parameters used for Figs. 4(a,b) correspond to a practical case involving a SiN waveguide coupled evanescently to a grating of pillars (similar to [21]), pump wavelengths compatible with rare-earth ion-doped fibers amplifiers ($\{\lambda_1, \lambda_2\} = \{1550, 1308\}$ nm), and a signal wavelength typical of color centers in diamond ($\lambda_s = 630$ nm). In our simulation, the duration of the pump is taken 10 times longer than the duration of the signal in order to ensure a

Optics EXPRESS

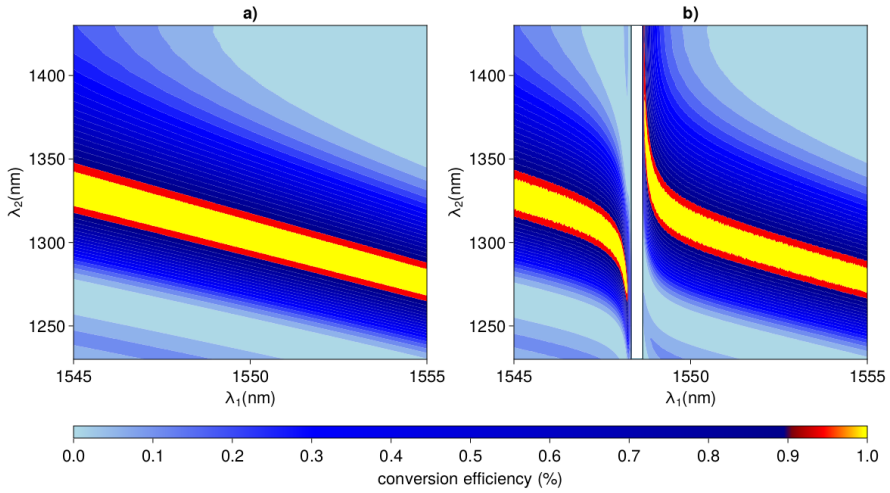

Fig. 4. BS-4WM efficiency in a waveguide (left) and in a waveguide Bragg grating (right) for the same set of wavelength. Horizontal axis stands for the first pump wavelength, while the vertical axis corresponds to the second pump wavelength. The color scale indicate the efficiency that belongs to [0,1], with red to yellow revealing an efficiency better than 0.9. The length of both systems is 1 cm and the Bragg wavelength is about 1548 nm. Vertical black lines indicate the bandgap edges and the bandgap has been blanked since only what happens when the pump is outside can be interpreted.

quasi constant pump power for the duration of the signal pulse. In the waveguide case (Fig. 4(a)), the tunability of λ_2 is roughly 30 nm at 1310 nm, with λ_1 being fixed at 1549 nm, while it is 70 nm for the grating case (Fig. 4(b)). If we allow λ_1 to vary by 1 nm, the tuning advantage is even more striking since it goes from 40 to 120 nm for the waveguide and grating case respectively. In that latter case, the same tuning in λ_1 allows for jumping from one side of the bandgap to the other, which translates into a greater tunability. This is done at the expense of a tiny spectral domain - the bandgap - that is no longer a working region for λ_1. Our model predicts the Bragg gratings can be used to enhance the tunability of the BS-4WM compared to the tunability in a similar waveguide. We will now apply our model to another case of interest.

3.4. *Grating assisted BS-4WM for noisefree wavelength conversion*

One of the application of BS-4WM consists in changing the wavelength of quantum light fields in a way that is both phase-preserving and noise free. For such applications, avoiding any process that may generate spectrally overlapping extra photons is essential. One such process is spontaneous four-wave mixing (Sp-4WM) as illustrated in Fig. 3(d). For the BS-4WM configurations illustrated in Figs. 3(a,b,e), the spontaneous four-wave mixing is usually irrelevant because it is spectrally well separated from the wavelengths of interest. However, there exist other BS-4WM configurations, as depicted in Fig. 5(a), where those quantum fields are in the close spectral vicinity of the pump beams and Sp-4WM depicted in Fig. 5(b)-c can become a strong source of noise. The presence of channel loss at the frequencies ν_{i2} and/or ν_{s2} may quench the spurious (i.e., undesired and concurrent) Sp4WM that would otherwise generate photons at the initial and final frequencies ν_s, ν_i of the BS-4WM. This is achieved without affecting the latter process as the loss and dispersive properties are restricted to wavelengths that are irrelevant to the desired BS-4WM. This loss channel can effectively be implemented with the reflection due to a Bragg grating [42]. The reflection of weak fields corresponds to $f \approx 0$ in Eq. (8), which

Optics EXPRESS

gives $|\kappa\frac{1-f^2}{2f}|>>|\gamma P\frac{1-f^2}{1+f^2}|$ that results in $q_{\text{total}} \approx q_{\text{linear}}$; all of the more in the moderate nonlinear regime with $\gamma PL \approx \pi/4<<\kappa L$ as in the following example.

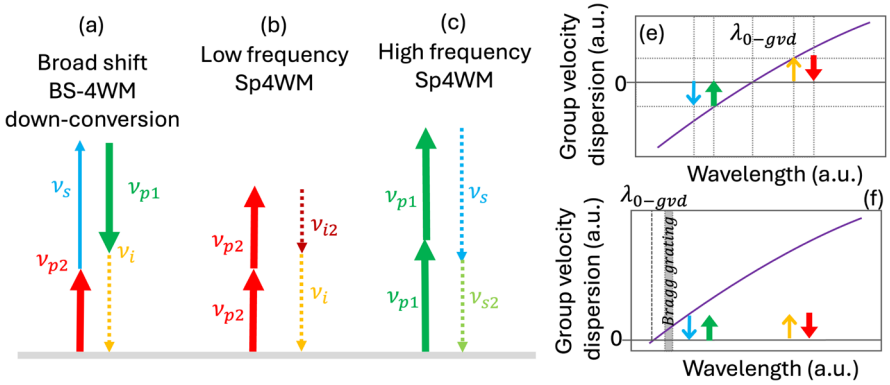

Fig. 5. Achieving noise-free large frequency translation via BS-4WM. (a) BS-4WM configuration allowing large frequency translation of the weak/quantum field from a frequency ν_s to the final frequency ν_i; (b,c) simultaneous spontaneous 4WM processes generating photons overlapping with the incident ν_s (c) and final ν_i (b) BS-4WM frequencies; (e) typical dispersion curve and relation to the BS-4WM process depicted in (a) [same colors as in (a)]; (f) dispersion configuration made possible via the presence of a Bragg grating to quench spurious Sp-4WM.

It is worth knowing that those spontaneous 4WM processes can be modeled by their classical counterpart: seeded four-wave mixing [43]. In the low gain regime ($\gamma PL<1$), the classical conversion efficiency between the seed and the newly generated wave being $\eta_{Sp} = P_{out}(\nu_{i2})/P_{in}(\nu_i)$ is indeed equivalent to the flux of spontaneous generated photons per mode (defined by the pump spectral-temporal profile); with $P_{out}(\nu_{i2})$ the output power at the frequency ν_{i2} and $P_{in}(\nu_i)$ the seeding input power at the frequency (ν_i) for the process of Fig. 5(b).

The numerical simulation of seeded 4WM and Bragg scattering can thus reveal the positive impact of the Bragg grating on the noise properties of the BS-4WM. Unlike coupled modes equations, this simulation accounts for the interplay between those processes and possibly complex dynamics. This is illustrated in Fig. 6. While four distinct Sp-4wm processes (Fig. 6(A-D)) may take place and add noise to BS-4WM processes of interest (Fig. 6(E-F)) when we use a simple waveguide, the presence of the Bragg grating suppresses the spurious phenomena, thus preserving the purity of the desired BS-4WM. In order to quantify this improvement, let us define the desired conversion efficiency via the process of Fig. 6(F) as $\eta_{F,f_{2-}} = P(f_{2-}, L)/P(f_{1-}, 0)$. The similarly defined conversion efficiencies associated to processes 6(A-D) correspond to the amount of spurious photons spontaneously generated [43]. We can thus also introduce an index of "impurity" as $\rho_F = \frac{(\eta_{C,f_{2-}}+\eta_{C,f_{1-}}+\eta_{D,f_{2-}}+\eta_{D,f_{1-}}+\eta_{F,f_{2-}})}{\eta_{F,f_{2-}}} - 1$. This quantity represents the total conversion and generation of photons to the initial and final frequency bins f_{2-} and f_{1-} via the processes A, B, C, D, F normalized by the desired conversion via the process F (a similar definition ρ_E can be made for the process E). The magnitude of ρ_F reaches 0 for a perfectly pure conversion (no added photon noise) and gets greater than one if the probability of generating a spurious photon exceeds the probability of converting the initial photon. In the waveguide case (Fig. 6(F)), the impurity is high at $\rho_F = 1.054$ while being strongly reduced to $\rho = 0.132$ in the presence of the grating thanks to the suppression of the spurious processes involved with f_{2+}. Interestingly, the symmetric scheme (Fig. 6(E)) presents very similar values (differing only to the 5th digit). The presence of the grating here improves the relevant figure of merit ρ by nearly an order of magnitude while adding absolutely no penalty.

Optics EXPRESS

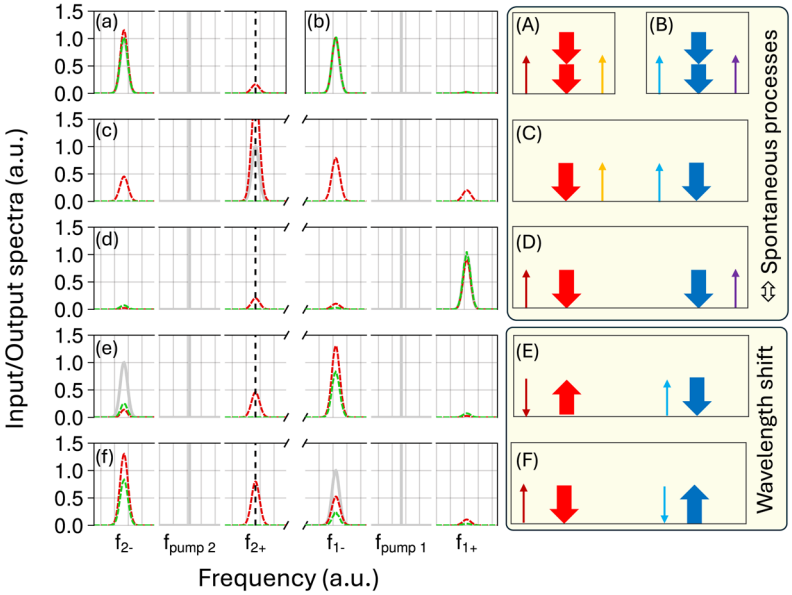

Fig. 6. Four-wave mixing output spectra in waveguides with (green curves) and without (red curves) the presence of a Bragg grating (vertical dotted line). The various plots differ by their input signal frequency (grey curves) and the presence of one (a-b) or two (c-f) pump beams. (a) pump-degenerate seeded four-wave mixing (as A) when only pump at $f_{\text{pump 2}}$ is on - the presence of the grating strongly quenches the process; (b) the same process (as B) in the vicinity of a pump at $f_{\text{pump 1}}$ is weak owing to a phase-mismatch; (c) when both pump beams are present the process of non-degenerate 4-wave-mixing (as C) competes and interplay with the 2 previous ones; (d) a similar situation involving process (D) can be observed when the signal is placed at the highest frequency; (e) the process of Bragg scattering four-wave mixing also may compete with all the previous processes unless a Bragg gratings quenches them. All sub plots are spanning 22 GHz and correspond to the following realistic configuration of a silicon nitride waveguide. The grating contrast is $\delta n_1 = 2.245 \times 10^{-4}$) and the length of the waveguide is $L = 2.5$ cm. The pump duration (800 ps) is taken much longer than the seed duration (200 ps) in order to maintain a quasi continuous profile over the duration of the seed. The pump beams have an identical power of 14 W to maximize the efficiency of the Bragg scattering process (e-f) [that is $\gamma PL \approx \pi/4$] while the seed are of much smaller power to satisfy the assumption of undepleted pump. The frequencies values are $f_{p1} = 418.50$ THz, $f_{p2} = 247.69$ THz, $f_{\pm X} = f_{pX} \pm 5.00$ THz with $X \in \{1, 2\}$.

3.5. *Tailoring the spectral waveform of photon pairs and heralded single photons*

If the grating allows for the strong quenching of Sp-4WM, it can also empower it. Especially, the Bragg grating allows for tailoring the spectral distribution of spontaneously generated photon pairs via that particular process (Fig. 5(b)). A highly desired configuration for photon pairs generation consists in having the Stokes (red-detuned) and anti-Stokes (blue-detuned) photons spectrally well separated from the pump and from each other. In this situation, the heralding (at λ_h) and heralded photon (at λ_t) can be separated spectrally without cutting in the spectral distribution. Moreover, by adjusting both the pump bandwidth and the phase matching bandwidth, indistinguishable photons can be generated [44] upon an heralded event. Such achievement is possible using four-wave mixing via fourth-order dispersion phase matching [45] or birefringence phase matching [46]. But these techniques are experimentally challenging to implement as they demand a high control of the dispersion or birefringence properties of the waveguide. Hereafter,

Optics EXPRESS

we show that a Bragg grating may help in reaching such a desired configuration while being rather easy to implement. Figure 7(left) shows the typical spectral density of spontaneous four-wave mixing in a 10cm-long waveguide that exhibits the typical $\mathrm{sinc}^2\left(\pi\beta_2\Delta f^2\right)$ dependence in the spectral detuning. Adding an evanescently coupled Bragg grating to the same waveguide, the sidebands can be detached from the pump frequency as seen in Fig. 7(right).

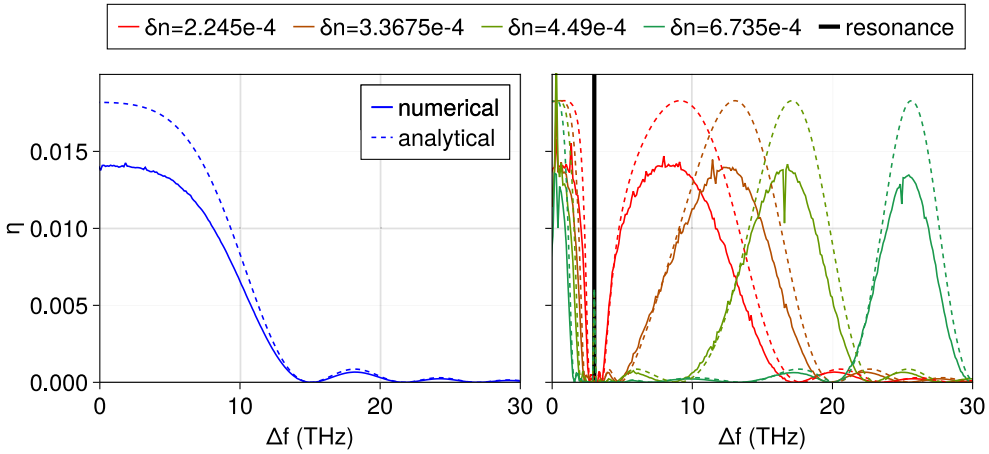

Fig. 7. Simulation of spontaneous pump degenerate 4WM in a waveguide (left) and a gratings (right) for several index modulation amplitudes as a function of the pump-signal detuning. The optimal bandwidth (maximum efficiency) is located in the immediate vicinity of the pump for the waveguide case whereas a detached sideband appears in the grating. The separation grows with the index modulation amplitude. The analytical (continuous wave) expectation (dash lines) overestimates the efficiency when the pump is pulsed (bold lines). Parameters of the simulation are: Pump wavelength is 915.85 nm, pulse duration 500 ps, nonlinear phase shift $\gamma PL = 0.135<1$, Bragg resonance at $\Delta f = 2.97$ THz.

The grating dispersion indeed influences the phase-matching which in turn changes the spectral location of efficient conversion. As expected, the separation is stronger for stronger gratings. An analytical description of the process in terms of phase-matching with a continuous pump gives a decent overview of the process. However, unlike our model, it fails at predicting the conversion efficiency value η when the pump is pulsed. The failure increases when the pump duration becomes shorter and shorter, as illustrated in Fig. 8, hence highlighting the importance of our procedure.

4. Conclusion and outlook

Encoding the grating behaviour upon the dispersion operator in the NLSE allows for having a single equation to model both Kerr nonlinearity and the grating dispersive effects, providing a low to mid intensity regime that is relevant to many applications. This equation is easily solved numerically, using the split-step Fourier algorithm, as the grating dispersion operator in the frequency domain has a direct expression. We have validated this approach by comparing it with known results that are usually modeled using coupled equations. Then we have used our model to provide new insights on a few applications that we find relevant and that exploit both the reflective or dispersive properties of the Bragg grating. Each of these applications would deserve a dedicated study that we leave for further inspection. However, our results demonstrate an undeniable range of improvements for pair generation and wavelength conversion.

Besides obvious experimental demonstrations, we hope our study will be further expanded to account for polarization effect and for allowing doubly resonant Bragg gratings. In integrated

Optics EXPRESS

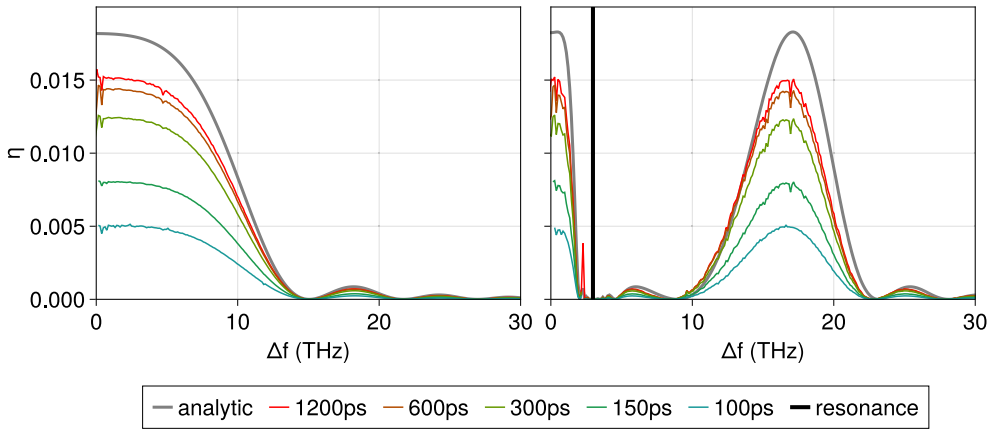

Fig. 8. Simulation of degenerate photon pair production rate (photon/Hz/s) in a waveguide (left) and a grating (right, with $\delta n = 4,49.10^{-4}$) for several pump durations (the signal duration is always 100 ps) as a function of the pump-signal detuning. The analytical (continuous wave) expectation is the gray line and overestimates the pair production when the pump beam is pulsed (colored lines). For all curves, the parameters are representative of the low gain regime suitable for photon pair production ($\gamma PL = 0.135$).

photonics, such gratings could be easily implemented by having two pillars of different periods coupled evanescently to a main waveguide. We also emphasize that our study could be generalized to other dispersive structures. Indeed, it eventually implies that the modeling of a one dimensional propagation in presence of a spectrally localized structure, only requires to have the linear transfer function of the system to adjust the dispersion operator, and to identify the moderate nonlinear to ensure the validity of the modeling. Hence, the behaviour of more complex gratings (like Moiré gratings) with a more complex dispersion operator relying on a z-dependent q may be explored in the future.

Funding. Fonds de la Recherche Scientifique - FNRS (MIS F.4506.20, EOS.40007526); Fonds pour la Formation à la Recherche dans l'Industrie et dans l'Agriculture.

Acknowledgment. Stéphane Clemmen is a research associate of the Fonds de la Recherche Scientifique (FNRS). Timothé David is a FRIA grantee of the Fonds de la Recherche Scientifique – FNRS

Disclosures. The authors declare no conflicts of interest.

Data availability. Data underlying the results presented in this paper are not all publicly available at this time but may be obtained from the authors upon reasonable request.

Supplemental document. See Supplement 1 for supporting content.

References

1. C. McKinstrie, J. Harvey, S. Radic, *et al.*, "Translation of quantum states by four-wave mixing in fibers," Opt. Express **13**(22), 9131–9142 (2005).
2. K. Bergman, H. Haus, E. Ippen, *et al.*, "Squeezing in a fiber interferometer with a gigahertz pump," Opt. Lett. **19**(4), 290–292 (1994).
3. D. M. Pepper, J. AuYeung, D. Fekete, *et al.*, "Spatial convolution and correlation of optical fields via degenerate four-wave mixing," Opt. Lett. **3**(1), 7–9 (1978).
4. R. Salem, M. A. Foster, A. C. Turner, *et al.*, "Optical time lens based on four-wave mixing on a silicon chip," Opt. Lett. **33**(10), 1047–1049 (2008).
5. G. P. Agrawal, *Nonlinear Fiber Optics* (Elsevier, 2013), Chap. 2, 10.
6. L. Chen, P. Li, H.-S. Liu, *et al.*, "Coupled-generalized nonlinear schrödinger equations solved by adaptive step-size methods in interaction picture," Chin. Phys. B **32**(2), 024213 (2023).
7. A. Z. Sakhabutdinov, V. I. Anfinogentov, O. G. Morozov, *et al.*, "Numerical method for coupled nonlinear schrödinger equations in few-mode fiber," Fibers **9**(1), 1 (2021).
8. R. Kashyap, *Fiber Bragg Gratings* (Elsevier, 2010), Chap. 1.

Optics EXPRESS

9. C. M. De Sterke, K. R. Jackson, and B. D. Robert, "Nonlinear coupled-mode equations on a finite interval: a numerical procedure," J. Opt. Soc. Am. B **8**(2), 403–412 (1991).
10. Z. Toroker and M. Horowitz, "Optimized split-step method for modeling nonlinear pulse propagation in fiber bragg gratings," J. Opt. Soc. Am. B **25**(3), 448–457 (2008).
11. F. Emami, M. Hatami, A. Keshavarz, *et al.*, "A heuristic method to simulate the pulse propagation in nonlinear fiber bragg gratings," Opt. Quantum Electron. **41**(6), 429–439 (2009).
12. B. J. Eggleton, C. M. de Sterke, and R. Slusher, "Nonlinear pulse propagation in bragg gratings," J. Opt. Soc. Am. B **14**(11), 2980–2993 (1997).
13. C. M. de Sterke and B. J. Eggleton, "Bragg solitons and the nonlinear schrödinger equation," Phys. Rev. E **59**(1), 1267–1269 (1999).
14. W. Chen and D. Mills, "Gap solitons and the nonlinear optical response of superlattices," Phys. Rev. Lett. **58**(2), 160–163 (1987).
15. C. M. de Sterke and J. Sipe, "Gap solitons," in *Progress in Optics*, vol. 33 (Elsevier, 1994), pp. 203–260.
16. B. J. Eggleton, R. Slusher, C. M. De Sterke, *et al.*, "Bragg grating solitons," Phys. Rev. Lett. **76**(10), 1627–1630 (1996).
17. G. P. Agrawal, *Applications of Nonlinear Fiber Optics* (Elsevier, 2001).
18. D. Tan, K. Ikeda, R. Saperstein, *et al.*, "Chip-scale dispersion engineering using chirped vertical gratings," Opt. Lett. **33**(24), 3013–3015 (2008).
19. C. Feng, L. Zhang, H. Luo, *et al.*, "Fast-light-assisted four-wave mixing in the photonic bandgap," Opt. Lett. **40**(12), 2790–2793 (2015).
20. M.-S. Kwon, "Quasi-phase-matched four-wave mixing enabled by grating-assisted coupling in a hybrid silicon waveguide," IEEE Access **10**, 83440–83451 (2022).
21. J. W. Choi, B.-U. Sohn, E. Sahin, *et al.*, "An optical parametric bragg amplifier on a cmos chip," Nanophotonics **10**(13), 3507–3518 (2021).
22. J. Knight, T. Birks, P. S. J. Russell, *et al.*, "All-silica single-mode optical fiber with photonic crystal cladding," Opt. Lett. **21**(19), 1547–1549 (1996).
23. M. R. Lamont, B. Luther-Davies, D.-Y. Choi, *et al.*, "Supercontinuum generation in dispersion engineered highly nonlinear (γ = 10/w/m) as 2 s 3 chalcogenide planar waveguide," Opt. Express **16**(19), 14938–14944 (2008).
24. R. Slusher, B. Yurke, P. Grangier, *et al.*, "Squeezed-light generation by four-wave mixing near an atomic resonance," J. Opt. Soc. Am. B **4**(10), 1453–1464 (1987).
25. A. Säynätjoki, M. Mulot, J. Ahopelto, *et al.*, "Dispersion engineering of photonic crystal waveguides with ring-shaped holes," Opt. Express **15**(13), 8323–8328 (2007).
26. A. Yariv, Y. Xu, R. K. Lee, *et al.*, "Coupled-resonator optical waveguide:? a proposal and analysis," Opt. Lett. **24**(11), 711–713 (1999).
27. M. Gagné, S. Loranger, J. Lapointe, *et al.*, "Fabrication of high quality, ultra-long fiber bragg gratings: up to 2 million periods in phase," Opt. Express **22**(1), 387–398 (2014).
28. E. Bernhardi, H. A. van Wolferen, L. Agazzi, *et al.*, "Ultra-narrow-linewidth, single-frequency distributed feedback waveguide laser in al_2o_3:Er^{3+} on silicon," Opt. Lett. **35**(14), 2394–2396 (2010).
29. P. Westbrook and J. Nicholson, "Perturbative approach to continuum generation in a fiber bragg grating," Opt. Express **14**(17), 7610–7616 (2006).
30. B. Fornberg, "On a fourier method for the integration of hyperbolic equations," SIAM J. Numer. Anal. **12**(4), 509–528 (1975).
31. C. J. McKinstrie, S. Radic, and A. R. Chraplyvy, "Parametric amplifiers driven by two pump waves," IEEE J. Sel. Top. Quantum Electron. **8**(3), 538–547 (2002).
32. G. P. Agrawal, *Applications of Nonlinear Fiber Optics* (Elsevier, 2008), Chap. 1.
33. P. Westbrook, J. Nicholson, K. Feder, *et al.*, "Supercontinuum generation in a fiber grating," Appl. Phys. Lett. **85**(20), 4600–4602 (2004).
34. D. Janner, G. Galzerano, G. Della Valle, *et al.*, "Slow light in periodic superstructure bragg gratings," Phys. Rev. E **72**(5), 056605 (2005).
35. T. David, "Grating dispersion operator nlse," https://github.com/Makhnobi/GratingDispersionOperatorNLSE (2025).
36. H. G. Winful, "Pulse compression in optical fiber filters," Appl. Phys. Lett. **46**(6), 527–529 (1985).
37. R. Campbell and R. Kashyap, "The properties and applications of photosensitive germanosilicate fiber," International J. Optoelectronics **9**, 33–57 (1994).
38. C. J. McKinstrie and M. G. Raymer, "Four-wave-mixing cascades near the zero-dispersion frequency," Opt. Express **14**(21), 9600–9610 (2006).
39. S. Clemmen, "Coherent frequency conversion for quantum information processing," in *Real-time Measurements, Rogue Phenomena, and Single-Shot Applications V*, vol. 11265 (SPIE, 2020), pp. 17–23.
40. I. Agha, M. Davanço, B. Thurston, *et al.*, "Low-noise chip-based frequency conversion by four-wave-mixing bragg scattering in sin x waveguides," Opt. Lett. **37**(14), 2997–2999 (2012).
41. J. B. Christensen, J. G. Koefoed, B. A. Bell, *et al.*, "Shape-preserving and unidirectional frequency conversion by four-wave mixing," Opt. Express **26**(13), 17145–17157 (2018).
42. L. Helt, A. M. Brańczyk, M. Liscidini, *et al.*, "Parasitic photon-pair suppression via photonic stop-band engineering," Phys. Rev. Lett. **118**(7), 073603 (2017).

Optics EXPRESS

43. L. G. Helt, M. Liscidini, and J. E. Sipe, "How does it scale? comparing quantum and classical nonlinear optical processes in integrated devices," J. Opt. Soc. Am. B **29**(8), 2199–2212 (2012).
44. F. Kaneda, K. Garay-Palmett, A. B. U'Ren, *et al.*, "Heralded single-photon source utilizing highly nondegenerate, spectrally factorable spontaneous parametric downconversion," Opt. Express **24**(10), 10733–10747 (2016).
45. M. R. Lamont, B. T. Kuhlmey, and C. M. de Sterke, "Multi-order dispersion engineering for optimal four-wave mixing," Opt. Express **16**(10), 7551–7563 (2008).
46. R. Tannous, P. J. Bustard, D. England, *et al.*, "Efficient quantum frequency translation of broadband single photons by bragg-scattering four-wave mixing," Opt. Quantum **3**(2), 168–174 (2025).